*Journal of Organometallic Chemistry*, 419 (1991) 375–382
Elsevier Sequoia S.A., Lausanne
JOM 22141

# A comparison of the energy barriers to bridge reversal in trisulphur- and triselenium-bridged [3]metallocenophanes

Edward W. Abel, Nicholas J. Long, Keith G. Orrell, Anthony G. Osborne and Vladimir Šik
*Department of Chemistry, The University, Exeter EX4 4QD (UK)*

(Received June 14th, 1991)

## Abstract

The [3]metallocenophanes with trichalcogen chains as bridging groups, namely $[M(C_5H_4E)_2E']$ (M = Ru, Os, E = E′ = S; M = Ru; E = E′ = Se), have been shown by NMR spectroscopy to be fluxional by a bridge reversal process. From two-dimensional NMR exchange experiments (2D-EXSY), accurate energy data for the bridge reversal fluxion have been obtained and compared with previous data for analogous [3]ferrocenophanes. The $\Delta G^{\ddagger}$(298 K) values for the process lie in the range 67–93 kJ $mol^{-1}$. Magnitudes increase in the order Fe < Ru < Os, reflecting the increasing strength of metal–ring bonding, and in the order $Se_3 < S_3$ due to the different torsional energies of the chalcogen–chalcogen bridge bonds.

## Introduction

The presence of a bridge reversal fluxion in [3]ferrocenophanes has been known for many years [1–4]. Early NMR studies provided only approximate estimates of the energy barriers involved. In a series of studies [5–7] we have applied total NMR bandshape methods to provide more accurate quantitative data for the energy barriers in all nine members of the 1,2,3-trichalcogena[3]ferrocenophanes, namely $[Fe(C_5H_4E)_2E']$ (E = E′ = S, Se, Te; E ≠ E′ = S, Se, Te). It was shown possible to relate the energies to the relative magnitudes of the torsions of the chalcogen–chalcogen single bonds in these pseudo-six-membered rings. We have now studied the compounds $[M(C_5H_4S)_2S]$ (M = Ru, Os) and $[Ru(C_5H_4Se)_2Se]$ with a view to measuring the dependence of the bridge reversal fluxion on the type of 'sandwich' metal, as this must influence the inter-ring distance and thus affect the bridgehead strain in these compounds. On account of the particularly slow rates of bridge reversal exhibited by these [3]ruthenocenophane and [3] osmocenophane compounds, the results we report herein are based on variable temperature two-dimensional NMR exchange experiments (2D-EXSY) rather than one-dimensional bandshape analyses as used for the [3]ferrocenophanes [5,6].

## Experimental

The following compounds were prepared by published literature methods: 1,2,3-trithia[3]ruthenocenophane [8], 1,2,3-triselena[3]ruthenocenophane [9], and 1,2,3-trithia[3]osmocenophane [10].

Hydrogen-1 NMR spectra were recorded on a Bruker AM 250 FT spectrometer operating at 250.13 MHz. The compounds were recorded as solutions in $CDCl_3$, $CD_2Cl_2$, $C_6D_6$ or $C_6D_5NO_2$, the choice depending on the compound and temperature range under investigation. Chemical shifts are quoted relative to $Me_4Si$ as an internal standard. A model B-VT100 variable temperature unit was used to control the sample temperature, and the temperature values are accurate to ±1°C.

Hydrogen-1 2D-EXSY spectra were recorded as previously reported [11,12] using the Bruker automation program NOESYPH to produce pure absorption mode spectra. In these 2D NMR experiments, both the F1 and F2 dimensions contained 256 words, the spectral width SW was 280 Hz and the mixing time, $\tau_m$, varied between 0.05 and 3.0 s depending on the compound and its spectral measurement temperature. The number of scans varied between 32 and 64. The data were processed using an exponential window function (line broadening of 1 Hz) in both dimensions and symmetrised about the diagonal. Auto- and cross-peak signal intensities were measured accurately by integrations of appropriate rows of the 2D data table. These were used as input data for the D2DNMR program [11] which computes first order rate constants on the assumption of negligible effects of nuclear cross-relaxation processes.

## Results

The bridge reversal conformational change in [3]ferrocenophanes with chalcogen bridging atoms is well-established and its rate can be monitored very precisely from its averaging effects on the ring methine proton NMR signals (Fig. 1) [5,7]. NMR bandshape analysis has established the dependence of the bridge reversal energy barrier on the nature of the chalcogen bridge atoms. We now report studies on ruthenium and osmium analogues of previously studied [3]ferrocenophanes in order to deduce the influence of the 'sandwich' metal on the bridge reversal rates.

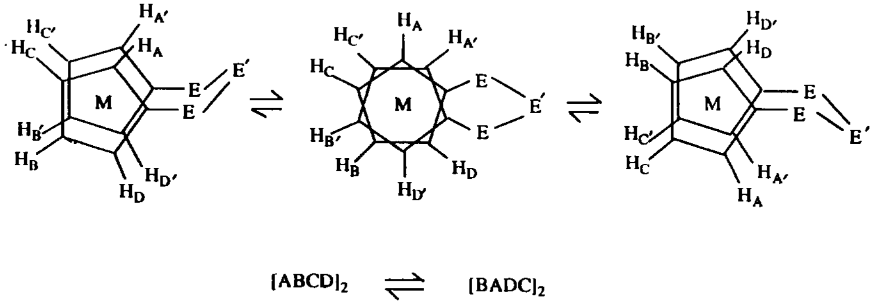

Fig. 1. Bridge reversal process in compounds $[M(C_5H_4E)_2E']$ (M = Fe, Ru, Os; E = E' = S, Se) showing the averaging effects on the ring methine environments.

### *[Ru($C_5H_4S$)$_2$S]*

The ambient temperature $^1H$ NMR spectrum of a solution in $C_6D_6$ consists of four sharp signals, exhibiting weak multiplet splitting, due to the four non-equivalent pairs of protons A/A′, B/B′, C/C′ and D/D′ as shown in Fig. 1. Two of the signals had very similar chemical shifts but were clearly resolvable. Following the previous work [5], signals 1 and 4 were assigned to protons A/A′ and D/D′ respectively, and signals 2 and 3 to protons B/B′ and C/C′. Due to the closeness of signals 2 and 3 a reversed assignment cannot be ruled out.

On raising the temperature of the solution, no significant changes were detected up to ca 100°C, showing that the rate of $S_3$ bridge reversal was still comparatively slow. It was clear that the process possessed too high an energy to be monitored by NMR bandshape analysis of exchange broadened signals, and attention was turned to the NMR 2D-EXSY method [11] which allows measurement of much slower rates of exchange. A 2D-EXSY spectrum at 60°C with a relatively long mixing time exhibited clear cross-peaks between the outer pair of methine signals, from which a first order rate constant for the bridge reversal process could be derived [11]. The other two methine signals had virtually merged at this temperature and therefore no kinetic information could be extracted from them. Further 2D-EXSY spectra were obtained at ten-degree intervals from 70 to 110°C inclusive, and further rate data calculated. A change of solvent from $C_6D_6$ to $C_6D_5NO_2$ was necessary above 90°C but this is unlikely to affect the rate data on account of the known intramolecular nature of the conformational process.

### *[Os($C_5H_4S$)$_2$S]*

The methine proton chemical shifts for this compound are given in Table 1. Proton NMR 2D-EXSY spectra were recorded on $C_6D_6$ or $C_6D_5NO_2$ solutions between 60 and 110°C. The 2D spectrum recorded at 90°C is shown in Fig. 2 with the 1D spectrum along the top edge of the contour plot. For the $C_6D_6$ solution spectra, rate constants were derived from the cross-peaks associated with both the inner and outer pairs of methine signals. Table 2 shows the good agreement obtained between the both sets of data.

### *[Ru($C_5H_4Se$)$_2$Se]*

The $^1H$ NMR spectra of this compound again showed four methine signals with the inner pair quite closely separated. Rates of reversal of the $Se_3$ bridge are expected to be appreciably faster than for the $S_3$ bridge [5]. Nevertheless, no signs

Table 1

$^1H$ NMR parameters for 1,2,3-trichalcogena[3]metallocenophanes

| Compound | Solvent | T/ °C | $\delta_1$ [a]/ppm | $\delta_2$ [a]/ppm | $\delta_3$ [a]/ppm | $\delta_4$ [a]/ppm | Ref. |
|---|---|---|---|---|---|---|---|
| [Fe($C_5H_4S$)$_2$S] | $C_6D_5NO_2$ | 60 | 3.62 | 4.18 | 4.26 | 4.32 | 5 |
| [Ru($C_5H_4S$)$_2$S] | $C_6D_6$ | 60 | 3.90 | 4.41 | 4.43 | 4.67 | This work |
| [Os($C_5H_4S$)$_2$S] | $C_6D_6$ | 60 | 4.08 | 4.56 | 4.63 | 4.85 | This work |
| [Fe($C_5H_4Se$)$_2$Se] | $C_6D_5CD_3$ | 60 | 3.55 | 3.79 | 3.81 | 4.05 | 5 |
| [Ru($C_5H_4Se$)$_2$Se] | $CDCl_3$ | 50 | 4.22 | 4.71 | 4.76 | 4.94 | This work |

[a] Chemical shifts rel. to $Me_4Si$ (int). All signals are weakly split into pseudo-quintets due to 3- and 4-bond couplings with other methine protons.

Table 2

Rate data derived from NMR 2D-EXSY spectra for the bridge reversal process in [3]metallocenophanes

| Compound | Solvent | $T/°C$ | $\tau_m$ [a]/s | $k$ [b]/$s^{-1}$ | |
|---|---|---|---|---|---|
| $[Ru(C_5H_4S)_2S]$ | $C_6D_6$ | 60 | 3.0 | 0.09 | |
| | $C_6D_6$ | 70 | 1.5 | 0.27 | |
| | $C_6D_6$ | 80 | 0.5 | 0.73 | |
| | $C_6D_6$ | 90 | 0.1 | 1.45 | |
| | $C_6D_5NO_2$ | 100 | 0.05 | 4.13 | |
| | $C_6D_5NO_2$ | 110 | 0.05 | 8.44 | |
| $[Os(C_5H_4S)_2S]$ | $C_6D_6$ | 60 | 3.0 | 0.03 [c] | 0.04 [d] |
| | $C_6D_6$ | 70 | 2.0 | 0.12 | 0.14 |
| | $C_6D_6$ | 80 | 1.5 | 0.36 | 0.36 |
| | $C_6D_6$ | 90 | 0.5 | 1.18 | 1.19 |
| | $C_6D_5NO_2$ | 100 | 0.1 | 2.45 | |
| | $C_6D_5NO_2$ | 110 | 0.05 | 4.10 | |
| $[Ru(C_5H_4Se)_2Se]$ | $CDCl_3$ | 10 | 3.0 | 0.06 | |
| | $CDCl_3$ | 20 | 2.0 | 0.25 | |
| | $CDCl_3$ | 30 | 0.4 | 0.75 | |
| | $CDCl_3$ | 40 | 0.5 | 1.95 | |
| | $CDCl_3$ | 50 | 0.05 | 6.15 | |
| | $CDCl_3$ | 60 | 0.02 | 14.5 | |

[a] Mixing time of 2D-EXSY pulse sequence. [b] Estimated accuracy ±1%. [c] Values based on outer pairs of methine cross-peaks. [d] Values based on inner pairs of methine cross-peaks.

of line broadenings were observed in the 1D $^1H$ spectra up to ca 60°C, so again the 2D-EXSY method was preferred. Spectra obtained in the temperature range 10–60°C using $CDCl_3$ as solvent contained clearly defined cross-peaks and rate data were calculated using the D2DNMR computer program (Table 2). The rate constants were based on the cross-peaks between signals 1 and 4. Cross-peaks between the closely separated pair of signals 2 and 3 were clearly seen but their integrated intensities were judged to be less reliable than those for the other pair of cross-peaks and so they were not included in the calculations.

## Discussion

The methine proton NMR chemical shifts for the three [3]metallocenophanes are collected in Table 1 together with earlier data for the 1,2,3-trithia- and 1,2,3-triselena-[3]ferrocenophanes [5]. The shifts are all somewhat lower than those for the parent sandwich compounds $Cp_2M$ ($M = Fe, Ru, Os$), [13], but show an analogous trend to higher $\delta$ values on changing the metal from Fe to Ru to Os, the increment for either change of metal being 0.15–0.35 ppm for the trisulphur series and 0.7–0.95 ppm for the triselenium series. In all cases the methine protons adjacent to the chalcogen lone pair (viz. protons A/A′ in Fig. 1) are significantly more shielded than the other ring protons.

The activation energy parameters for the bridge reversal process are given in Table 3, previous data on analogous [3]ferrocenophanes being included for comparison purposes. In all cases, the $\Delta S^‡$ values are not considered to be of great

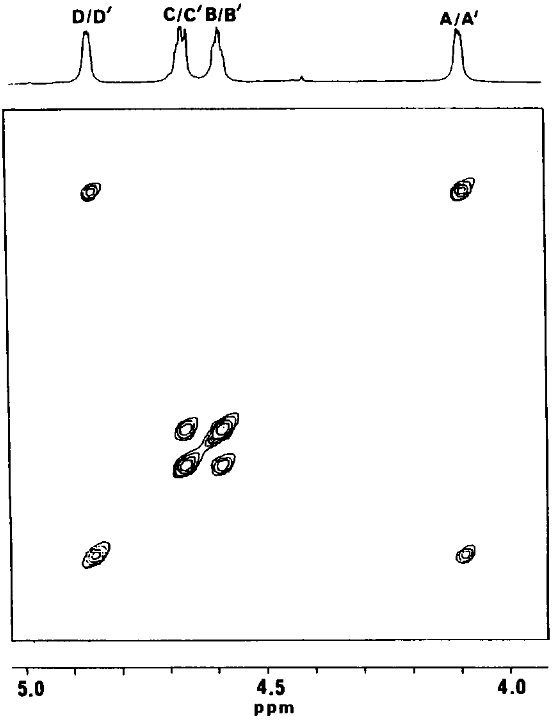

Fig. 2. The $^1H$ NMR 2D-EXSY spectrum of $[Os(C_5H_4S)_2S]$ at 90°C in $C_6D_6$ solution showing the exchange cross-peaks between both pairs of ring methine protons ($\tau_m = 0.05$ s).

significance, their near-zero magnitudes (in most cases) being simply indicative of a purely intramolecular rearrangement. The $\Delta G^{\ddagger}$ values, which are most representative of energy barrier trends range widely from 52 kJ mol$^{-1}$ (for $[Fe(C_5H_4Te)_2Te)]$) to 93 kJ mol$^{-1}$ (for $[Os(C_5H_4S)_2S]$). In the 1,2,3-trithia-bridged compounds, energies increase with the mass/size of the sandwich metal, namely Fe < Ru < Os. A similar trend is noted in the triselena-bridged compounds with Fe < Ru. For both series the energy increment in replacing Fe by Ru is ca 8 kJ mol$^{-1}$, while for the $S_3$ series the increment for replacement of Ru by Os is only ca 4 kJ mol$^{-1}$.

Further examination of the $\Delta G^{\ddagger}$ data in Table 3 shows that the bridge reversal process is more sensitive to a change of chalcogen bridge atom than to a change in

Table 3

Arrhenius and Eyring activation parameters for bridge reversal in [3]metallocenophanes $[M(C_5H_4E)_2E']$

| M | E | $E_a$/kJ mol$^{-1}$ | $\log_{10}(A/s^{-1})$ | $\Delta G^{\ddagger\,a}$/kJ mol$^{-1}$ | $\Delta H^{\ddagger}$/kJ mol$^{-1}$ | $\Delta S^{\ddagger}$/J K$^{-1}$ mol$^{-1}$ | Ref. |
|---|---|---|---|---|---|---|---|
| Fe | Te | 63.7 ± 1.2 | 14.9 ± 0.2 | 51.8 ± 0.2 | 61.5 ± 1.2 | 33 ± 5 | 7 |
| Fe | Se | 68.4 ± 2.4 | 13.0 ± 0.4 | 67.2 ± 0.1 | 65.8 ± 2.4 | −5 ± 8 | 5 |
| Ru | Se | 86.0 ± 2.1 | 14.7 ± 0.4 | 75.3 ± 0.1 | 83.4 ± 2.1 | 27 ± 7 | This work |
| Fe | S | 80.3 ± 0.9 | 12.7 ± 0.1 | 80.4 ± 0.2 | 77.0 ± 0.9 | −12 ± 2 | 5 |
| Ru | S | 95.5 ± 2.1 | 14.0 ± 0.3 | 88.8 ± 0.4 | 92.6 ± 2.1 | 12 ± 6 | This work |
| Os | S | 109.2 ± 7.4 | 15.6 ± 1.1 | 92.9 ± 1.2 | 106.3 ± 7.5 | 45 ± 21 | This work |

[a] At 298.15 K.

'sandwich' metal. For example, changing from an $S_3$ to a $Se_3$ bridge lowers the barrier by 13.2 kJ mol$^{-1}$ in the case of the ferrocenophanes and by 13.5 kJ mol$^{-1}$ in the case of the ruthenocenophanes. The change from an $Se_3$ to a $Te_3$ bridge in the ferrocenophane series causes a greater energy decrease of 15.4 kJ mol$^{-1}$. Such trends are not unexpected and reflect the relative magnitudes of torsional energies of chalcogen-chalcogen bonds, namely Te–Te < Se–Se < S–S [5,7].

In a recent study [7], we provided theoretical evidence in support of a bridge reversal mechanism which involves a transition state structure with staggered $C_5$ rings (Fig. 1), rather than one with eclipsed $C_5$ rings and a planar C–E–E′–E–C bridge. For such a structure to be attained, relative rotation of the two $C_5$ rings must occur, and the ease with which this happens will be a function of the strength of the ring–metal–ring bonding. There are numerous pieces of evidence which point to the strength of metal-ring bonding in the parent metallocenes $Cp_2M$ increasing in the order Fe < Ru < Os. Electrophilic reactivities of these compounds decrease in the order Fe > Ru > Os, and this is attributed to tighter ring-to-metal bonding resulting in lower $\pi$-electron density around the rings [14]. IR spectra of metallocenes exhibit low wavenumber shifts of C–C stretching and C–C ring breathing modes [15], and high wavenumber shifts of ring–M–ring symmetrical stretching modes [16], with increasing size of the metal. This is interpreted as evidence of weakening of C–C bonding in the Cp rings and a strengthening of ring metal bonding. More recent Raman studies have led to force constants for the Cp–M bond being in the order Cp–Fe < Cp–Ru < Cp–Os [17]. There is therefore a body of evidence to support the present finding that in 1,2,3-trichalcogena[3]metallocenophanes the transition state structure with staggered $C_5$ rings will be most easily achieved when iron is the sandwich metal and least easily achieved with osmium, with the ring–Os–ring bonding causing considerable resistance to relative rotation of the $C_5$ rings.

The total range of bridge reversal energies for all 1,2,3-trichalcogena[3]metallocenophanes will clearly be a function of the metal-ring bonding strength, the geometry of the C–E–E′–E–C bridge and the torsional energies of the E–E′ bonds. It was thought that such factors might be able to be represented by a single parameter such as the inter-ring distance (measured by the through space E ··· E distance) or the total bridge length. The appropriate values were taken from X-ray crystal data of six of these compounds and collated in Table 4. However, neither

Table 4

Bridge reversal energies and geometric parameters of [3]metallocenophanes, $[M(C_5H_4E)_2E']$

| M | E | $\Delta G^{\ddagger}$/kJ mol$^{-1}$ | E ··· E/pm | Bridge length [a]/pm | $E\hat{E}'E$ ground state | $E\hat{E}'E$ transition state | $\Delta E\hat{E}'E$ | Ref. [b] |
|---|---|---|---|---|---|---|---|---|
| Fe | Te | 51.8 | 395 | 973 | 91.6 | 109.9 [c] | 18.3 | 18 |
| Fe | Se | 67.2 | 356 | 850 | 100.7 | 117 [c] | 16.3 | 19 |
| Ru | Se | 75.3 | 362 | 846 | 102.15 | | | 9 |
| Fe | S | 80.4 | 323 | 759 | 103.9 | 125 [c] | 21.1 | 20 |
| Ru | S | 88.8 | ? | ? | 105.8 [d] | | | |
| Os | S | 92.9 | 328 | 761 | 106.4 | | | 10 |

[a] Length of C–E–E′–E–C bridge. [b] References for E ··· E distances and $E\hat{E}'E$ angles based on X-ray data. [c] From reference 7. [d] Interpolated value from graph (Fig. 3).

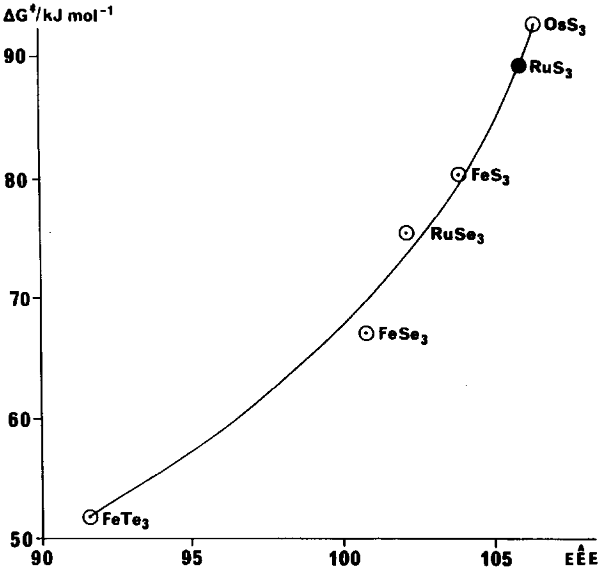

Fig. 3. The dependence of the bridge reversal energy ($\Delta G^{\ddagger}$/kJ mol$^{-1}$) on the chalcogen bridgehead angle EÊ'E. The point (●) for [Ru($C_5H_4S$)$_2$S] is interpolated.

parameter shows any correlation with the bridge reversal energies. On the other hand, the bridgehead chalcogen angles, EÊ'E, do appear to show a definite but non-linear correlation with the bridge reversal energies (Fig. 3). No X-ray data are available for the compound [Ru($C_5H_4S$)$_2$S] but the graph allows a realistic estimate to be made of the EÊ'E angle in this compound.

A more pertinent correlation of bridge reversal energies would be with the difference between the EÊ'E angles in the ground and transition state structures of these compounds. EÊ'E angles for the staggered ring transition state structures of the three [3]ferrocenophanes have been calculated previously [7] by the CNDO/2 method and are included in Table 4. However, their precise magnitudes should be treated with caution as they are based on calculations which assumed that all the compounds adopted fully staggered ring geometries in the transition state with no changes in bond lengths during the whole ring reversal process. The expected correlation of bridge reversal energies increasing with the extent to which the EÊ'E angle increases from the ground state to the transition state (i.e. ΔEÊ'E) appears to be valid for [Fe($C_5H_4S$)$_2$S] compared to either [Fe($C_5H_4Se$)$_2$Se] or [Fe($C_5H_4Te$)$_2$Te], but the correlation fails when comparing the latter two compounds. We suspect that this is symptomatic of the lack of precision of the CNDO/2 based EÊ'E values and that such a correlation of $\Delta G^{\ddagger}$ values with ΔEÊ'E values is a realistic rationalisation of the trends in bridge reversal energies. However, more reliable structural data are clearly necessary in order to confirm and extend this correlation.

## References

1 M. Rosenblum, A.K. Banerjee, N. Danieli, R.W. Fish and V. Schlatter, J. Am. Chem. Soc., 85 (1963) 316.

2 T.H. Barr and W.E. Watts, Tetrahedron, 24 (1968) 6111.
3 A. Davison and J.C. Smart, J. Organomet. Chem., 19 (1969) P7.
4 A. Davison and J.C. Smart, J. Organomet. Chem., 174 (1979) 321.
5 E.W. Abel, M. Booth and K.G. Orrell, J. Organomet. Chem., 208 (1981) 213.
6 E.W. Abel, M. Booth, C.A. Brown, K.G. Orrell and R.L. Woodford, J. Organomet. Chem., 214 (1981) 93.
7 E.W. Abel, K.G. Orrell, A.G. Osborne, V. Šik and W. Guoxiong, J. Organomet. Chem., 411 (1991) 239.
8 S. Akabori, H. Munegumi, Y. Habata, S. Sato, K. Kawazoe, C. Tamura and M. Sato, Bull. Chem. Soc., Jpn., 58 (1985) 2185.
9 A.J. Blake, R.O. Gould and A.G. Osborne, J. Organomet. Chem., 308 (1986) 297.
10 E.W. Abel, N.J. Long, A.G. Osborne, M.B. Hursthouse and M.A. Mazid, J. Organomet. Chem., to be published.
11 E.W. Abel, T.P.J. Coston, K.G. Orrell, V. Šik and D. Stephenson, J. Magn. Reson., 70 (1986) 34.
12 E.W. Abel, I. Moss, K.G. Orrell, V. Šik and D. Stephenson, J. Chem. Soc., Dalton Trans., (1987) 2695.
13 G. Wilkinson, F.G.A. Stone and E.W. Abel (Eds.), Comprehensive Organometallic Chemistry, Vol. 4, Pergamon Press, Oxford, 1982, pp. 478, 761, 1018.
14 M.D. Rausch, E.O. Fischer and H. Grubert, Inorg. Chem., 82 (1960) 76.
15 E.R. Lippincott and R.D. Nelson, J. Am. Chem. Soc., 77 (1955) 4990.
16 E.R. Lippincott and R.D. Nelson, Spectrochim. Acta, 10 (1958) 307.
17 B.V. Lokshin, V.T. Aleksanian and E.B. Rusach, J. Organomet. Chem., 86 (1975) 253.
18 M. Herberhold, P. Leitner and U. Thewalt, Z. Naturforsch, Teil B, 45 (1990) 1503.
19 S.H. Lockhart, M.Sc. Thesis, 1984, University of Virginia (private communication).
20 B.R. Davies and I. Bernal, J. Cryst. Mol. Struct., 2 (1972) 107.